- ... Steve Long's computer dated 07/31/02 12.24pm named "Preliminary SSA RAI Response.PDF"

PRELIMINARY

RESPONSES TO
NRC STAFF COMMENTS AND QUESTIONS ON DAVIS-BESSE SAFETY SIGNIFICANCE ASSESSMENT (SIA-W-DB-01Q-301) SUBMITTED APRIL 8, 2002

Question 1
What is the technical basis of the failure criterion (e.g., strain exceeding 11.15%) used to determine the failure conditions of the cladding layer? Provide specific technical references in the literature that support the failure criterion used in this evaluation.

Response to Question 1
The strain value of 11.15% corresponds to the uniform elongation of the stress-strain curve used in the evaluation. The use of this value as the basis for the failure criteria is based largely on engineering judgment. The premise is that when any section in the cladding has through-wall strains greater than the uniform elongation, then that section has no more capacity of resisting any additional increase in load. This criterion is judged to be conservative because in reality, there is redistribution of stresses and strains to adjacent elements that would prevent incipient failure when the strains in a particular column of elements exceed this criterion.

Furthermore, it should be noted that the value of uniform elongation used in the evaluation (11.15%) is very conservative for stainless steel weld metal. Data obtained from the literature, and summarized in Table 1 indicates that the average uniform elongation for submerged arc welds (SAW) is 25.7% and that for shielded metal arc welds (SMAW) is 30.7%. The average for both populations is 27.3%. Most of the data shown in Table 1 indicate uniform elongation greater than 20% with only two data points below this value.

Subsequent to the publication of SI Calculation W-DB-01Q-301, the above criterion has been used in a finite element analysis of disk specimens that were burst tested and documented in Reference 1. The geometry of the disk test specimens is very similar to the Davis-Besse RPV wastage cavity. The results of the evaluation are detailed in the Reference 2 calculation (attached). The conclusion from the Reference 2 analysis is that the present criterion used for the evaluation is conservative compared to the disk burst test results. The burst test pressures were also compared to the pressures at which numerical instability occurred during the elastic-plastic analysis and it was found that the instability pressures, although slightly under-predicting the test failure pressures, are a much better predictor of failure pressure than any of the proposed strain-based failure criteria.

Based on the above discussions, it is believed that the use of the 11.15% uniform elongation as a basis for the failure criterion is very conservative.

Question 2
How does the failure criterion (e.g., based on ultimate strain in a uniaxial tensile test) account for the effects of biaxial loading in the cladding, or triaxial loading in the cladding at the edges of the degradation cavity?

Response to Question 2
The failure criterion was based solely on the uniform elongation and did not consider biaxial or triaxial effects. Nevertheless, as discussed in the response to Question 1, the criterion is conservative compared to burst tests results on test specimens that are a reasonable simile of the wastage cavity geometry.

8/1/12

PRELIMINARY

Question 3
The failure criterion applied in SIA report W-DB-01Q-301 (e.g., the minimum cross-sectional strain exceeding the failure strain of 11.15%) allows the strain levels in the cladding to exceed the critical strain value entirely through the thickness, leading to very large strains at the surface of the cladding, up to 49% in Table 5 of the SIA report. What is the technical basis for this approach, as opposed to the average cross-sectional strain, or the maximum cross-sectional strain?

Response to Question 3
Even though the failure criterion used resulted in some elements in the cross-section exceeding the failure strain, the criterion, as compared to actual test data, was found to be conservative (see response to Question No.1)

Question 4
Did you explore a continuum damage mechanics analysis to give guidance of the failure criterion once the strains exceed the critical strain where necking/void growth starts? If not, provide the technical basis for not using a continuum damage mechanics analysis. [Poisson's ratio of 0.5 no longer applies once this critical strain level is exceeded, so the analysis is strictly not valid. (Poisson's ratio is continuously changing as the voids grow at the strains beyond the start of necking.) This results in a stress redistribution that is not accounted for in a standard elastic-plastic analysis.

Response to Question 4
The analysis performed was judged to be conservative as validated by the disk burst test results discussed in the response to Question 1, and as such, it was judged unnecessary to consider the application of continuum damage mechanics analysis to this evaluation.

Question 5
How would the strain values change if the stress free temperature was assumed to be the stress relief temperature instead of 70F, and the analysis accounted for the differential thermal expansion of the cladding and head steel at the operating temperature of 605F?

Response to Question 5
As can be seen in the SI report W-DB-01Q-301, and as further clarified by the above responses to Questions 1 through 4, the strains at the failure pressures from both the analyses and experiments are very large (on the order of 11% or greater). The strains corresponding to thermal expansion effects, at either temperature, are expected to be much smaller (on the order of 0.1%). Therefore, the effects of changing from a stress free temperature of 70F to 605F will not have any significant impact on the results of the analysis

Question A
Does the size of the degradation cavity and the transition from the cladding thickness to the head thickness that was used in the SIA report reflect current knowledge regarding the cavity geometry, in particular the undercut area described in Figure 13 on page 103 of the Davis-Besse Root Cause Analysis Report (CR2002-0891), dated April 15, 2002? What is the transition geometry assumed in the analyses?

Response to Question A
The size of the degradation cavity and the transition from the cladding thickness to the head thickness used in the calculation reflected what was the best available at the time of the calculation. More work is currently in progress on the removed damaged cavity to determine the exact size and geometry of the cavity and the transition regions.

Question B
Is there sufficient mesh refinement through the cladding thickness to adequately capture the bending and shear strains at the edge of the cavity? Describe any sensitivity studies used to demonstrate the adequacy of the mesh refinement.

Response to Question B
In the analysis of the wastage cavity, six elements were used through the thickness of the cladding. A convergence study, using both an axisymmetric model and a three dimensional model was performed in Reference 2 to evaluate the impact of the number of through-wall elements in the thickness of the test specimens. The results indicate that there is no significant difference in the burst pressure predictions when the number of through-wall elements is increased from six to 12. Therefore, it is concluded that the analyses of the wastage categories with six elements through the thickness represents a converged solution. Furthermore, when fewer elements than six were used in the convergence study, it resulted in conservative estimates of the burst pressures.

Question C
Was the cladding deposited by weld wire? Do the thinner cladding thickness measurements from UT coincide with the locations of weld bead toes? In what direction do the cladding weld beads run relative to the long axis of the degradation cavity?

Response to Question C
The cladding was deposited by weld wire. It is difficult to determine if the thinner cladding thickness measurements from the UT coincided with the location of the weld bead toes since the UT measurements were taken on one-inch grids and as such, there was not adequate resolution to make such a determination. It is also difficult to determine the direction of the cladding weld beads from the available information. Additional investigation of the removed damaged cavity is currently in progress that might provide more information

PRELIMINARY

References

1) P. C. Riccardella, "Elastic-Plastic Analysis of Constrained Disk Burst Tests," ASME Paper No. 72-PVP-12, Proceedings of Pressure Vessel and Piping Conference, New Orleans, LA, September 17-21, 1972.

2) Structural Integrity Calculation W-DB-01Q-304, Rev. 0, "Evaluation of Failure Criterion Used in Elastic-Plastic Analysis of Davis-Besse RPV Head Wastage."

PRELIMINARY

Table 1: Tensile Test Data for 304 Stainless Steel at 550°F

Reference	YS ksi	UTS ksi	Elong %	RA %	Matl Type
NUREG/CR-6235	20.8	62	38.4	70.8	Base
NUREG/CR-4538	22.2	67.3	39	70.8	Base
NUREG/CR-4538	22.8	68 8	40.5	70.8	Base
NUREG/CR-4687	20 1	65.2	53.8	71.3	Base
EPRI NP-4768	23.1	61.3	47	74	Base
EPRI NP-4768	24.8	62.6	45	70	Base
EPRI NP-4768	33.2	72.7	42	67	Base
ASME 72PVP12	34	84	54	75	Base
		Ave.Base	**45.0**	**71.2**	
EPRI NP-4668	44.8	62.9	22	46	SAW
EPRI NP-4768	36	61.8	25	67	SAW
EPRI NP-4768	40.8	70.3	25	69	SAW
NUREG/CR-6098	37.4	68	26.4		SAW
NUREG/CR-6389	49.1	68.1	30	46	SAW
NUREG/CR-6389	45	67.1	33	42.4	SAW
NUREG/CR-6389	54.3	74	15.5	63	SAW
NUREG/CR-6389	51.8	71.8	13.7	54	SAW
NUREG/CR-4878	471	67.6	31.5	44.2	SAW
NUREG/CR-4878	28.3	67.5	34.5	47	SAW-Ann
		Ave.SAW	**25.7**	**53.2**	
EPRI NP-4668	45.7	65.1	26	58	SMAW
EPRI NP-4768	46 8	61.4	37	48	SMAW
EPRI NP-4768	49 4	64.7	35	46	SMAW
NUREG/CR-4878	40.8	70.3	24.8	68 6	SMAW
		Ave.SMAW	**30.7**	**55.2**	
NUREG/CR-4538	44.3	65 4	33	74.3	Weld
NUREG/CR-4538	42.2	64.3	30	72.9	Weld
		Ave.SAW&SMAW	**27.3**	**53.8**	

PRELIMINARY

STRUCTURAL INTEGRITY Associates, Inc.	**CALCULATION PACKAGE**	**FILE No:** W-DB-01Q-304 **PROJECT No:** W-DB-01Q

PROJECT NAME: Operability and Root Cause Evaluation of the Damage of the Reactor Pressure Vessel Head at Davis-Besse

CLIENT: First Energy Corporation

CALCULATION TITLE: Evaluation of Failure Criterion Used in Elastic-Plastic Analysis of Davis-Besse RPV Head Wastage

PROBLEM STATEMENT OR OBJECTIVE OF THE CALCULATION:

Develop a finite element model to simulate actual test data to evaluate the effectiveness of the failure criteria used in the elastic-plastic stress analysis of Davis-Besse RPV head wastage cavity.

Document Revision	Affected Pages	Revision Description	Project Mgr. Approval Signature & Date	Preparer(s) & Checker(s) Signatures & Date
0	1 – 28 A1 – A2 B1 – B9 Project CD-Rom	Original Issue		

1.0 Introduction

During recent in-service inspections of the reactor pressure vessel (RPV) head and penetrations at Davis-Besse, significant wastage was observed in the vicinity of control rod drive mechanism (CRDM) No. 3. A calculation package was prepared for First Energy [1] to determine the limiting pressure load of the damaged RPV head.

Based on the review of this calculation package, the NRC raised a number of questions (See Appendix A), the majority of which were concerned with the failure criteria used in the evaluations.

The purpose of this calculation is to develop a better understanding of the failure criteria as used and its relative "conservativeness" in regards to the failure pressure.

2.0 Technical Approach

The failure criterion used in Reference 1 was set such that the maximum strain could not exceed the ultimate tensile strain. Hence for the stainless steel cladding where the maximum strain is expected to occur, the maximum equivalent total strain is limited to the maximum strain of 11.15% (corresponding to the ultimate strain for the stainless steel cladding in Reference 2) through the thickness of the component.

In order to evaluate the reasonableness of this failure criterion, the results of the failure pressures predicted with this criterion were compared against test results of very similar geometries. Disk burst test, similar to the Davis-Besse head wastage geometry were performed under the auspices of the PVRC Subcommittee and documented in and ASME publication [3] (see Appendix B for the actual publication).

Described in Reference 3 were a series of burst tests using machined disks of various materials. The test disk dimensions and the illustration of the test setup are shown in Figure 1. The materials tested included 304 Stainless Steel, A-533 Grade B Low Alloy Steel and A85 Grade C Carbon Steel. For the purposes of this calculation, only the 304 Stainless Steel testing will be reviewed.

As can be seen in Figure 1, three basic disk geometries were tested. In order to evaluate the effectiveness of the failure criteria developed for Reference 1, the same failure criteria will be used to determine the disk burst pressures. As a result, a series of finite element models were developed using the test disk dimension provided in Reference 3. The models were created and evaluated using the ANSYS finite element software [4]. The actual evaluations and subsequent failure criteria comparison are included in the following sections.

3.0 Finite Element Models

A series of finite element models were constructed to determine burst pressure for the various disk configurations. Initial studies were performed using an axisymmetric model but subsequent evaluations included three-dimensional modeling similar to that used in Reference 1.

The elastic material properties for all evaluations were for 304 stainless at room temperature as defined by Reference 5. These values used were as follows:

Modulus of Elasticity, E, e^6 psi:	28.3
Poisson's Ration, ν:	0.3

The plastic material properties for stainless per Reference 3 were:

0.25 Y.S. (psi)	**S_{ult} (psi)**	**ε_{ult} (in/in)**	**Reduction In Area**	**A[1] (psi)**	**n[1]**
34,000	84,000	0.54	0.74	193,060	0.494

[1] Stress Strain Curve Assumed to be of form $\sigma = A\,(\varepsilon)^n$

Therefore the stress-strain curve used in all of the evaluation is shown in Table 1. Any additional model specific conditions will be described in the following sections.

Table 1
Stress Strain Curve for 304 Stainless Steel [3]

Strain (in.in)	Stress (psi)
0 000	0
0.025	31208 63
0 050	43952.49
0 075	53699.79
0 100	61900 24
0 125	69113 97
0 150	75627.79
0 175	81611.83
0 200	87176 84
0.225	92399 68
0.250	97336 26
0 275	102028 8
0 300	106510
0 325	110805.8
0 350	114937.5
0.375	118922.4
0 400	122775
0 425	126507.5
0 450	130130 6
0 475	133653 1
0 500	137083
0 525	140427 1
0 550	143691.6
0 575	146881.9
0.600	150002 7
0 625	153058 4
0 650	156052 8
0 675	158989.5
0 700	161871.6
0 725	164702 2
0 750	167483.7
0.775	170218 7
0 800	172909.5
0.825	175558
0 850	178166 2
0 875	180735 8
0 900	183268 6
0 925	185766
0 950	188229.5
0 975	190660 4
1 000	193060
1 025	195429 4
1.050	197769.7
1 075	200082
1 100	202367.3
1 125	204626 4
1.150	206860 2
1.175	209069 7
1 200	211255 4
1.225	213418 2

3.1 Axisymmetric Finite Element Model

The axisymmetric models were developed in ANSYS using the 2-D 8-Node Structural Solid element, PLANE82. All three geometries described in Reference 3 were evaluated as was the effects of the finite element mesh density on the onset of numeric instability. A total of 5 evaluations for each disk geometry were made, the only difference between each evaluation was the mesh density, which can be simplified to the number of elements through the thickness of the thinned portion of the disk. As such, the mesh densities that were evaluated where 4, 6, 8, 10 and 12 elements through the thickness. Figure 2 shows the progression of mesh density for geometry-A.

The mechanical boundary conditions for these evaluations consisted of simple vertical restraint throughout the approximate clamp region. This region was assumed to into the entire region of the disk, which remained at the full 1 inch thickness. See Figure 3 for an example of the applied boundary conditions on the 4 element through thickness, geometry-A model.

3.2 Three-Dimensional Finite Element Model

The three-dimensional models were developed in ANSYS using the 3-D 8-Node Structural Solid element, SOLID45. All three geometries described in Reference 3 were evaluated as was the effects of the finite element mesh density on the onset of numeric instability.

Only a 30° section of the total disk was modeled since the loading and geometries were also symmetrical. Two evaluations for each disk geometry were made; the only difference between each evaluation was the mesh density, which again can be simplified to the number of elements through the thickness of the thinned portion of the disk. As such, the mesh densities for the 3-dimensional models that were evaluated were 4 and 6 elements through the thickness. It should be noted that the stainless clad for the actual Davis-Besse cavity evaluation used 6 elements through the thickness. Figure 4 shows the two mesh densities for geometry-A.

The mechanical boundary conditions for these evaluations used the same vertical restraints as the axisymmetric evaluations. In addition, axisymmetric boundary conditions were applied to the free ends of the disk, the preventing translations in the circumferential direction. This results in the centerline of nodes being limited to translation in only the vertical direction See Figure 5 for an example of the applied boundary conditions on the 4 element through thickness, geometry-A model.

4.0 Loading

All of the evaluations were loaded in the same manner. An incremental pressure was applied to the cavity surfaces until numeric instability was reached. See Figure 6 for an example of the applied pressure.

5.0 Mesh Density Results

For each evaluation, the pressure was allowed to rise incrementally until numeric instability occurred. The points of instability, as compared to the actual disk burst tests, are shown in Table 2.

Table 2
Mesh Density Effects of Numeric Instability

Model		Pressure (psi)		Predicted/ Test Result (%)
Model Type	Through-Wall Elements	Numeric Instability	Actual Test Burst	
Geometry A Models				
Axisymmetric	4	12725	15000	84.8
Axisymmetric	6	13942		92.9
Axisymmetric	8	14004		93.4
Axisymmetric	10	14022		93.5
Axisymmetric	12	14005		93.4
3-Dimensional	4	13979		93.2
3-Dimensional	6	13997		93.3
Geometry B Models				
Axisymmetric	4	5929	6800	87.2
Axisymmetric	6	6630		97.5
Axisymmetric	8	6695		98.5
Axisymmetric	10	6695		98.5
Axisymmetric	12	6694		98.4
3-Dimensional	4	6688		98.4
3-Dimensional	6	6671		98.1
Geometry C Models				
Axisymmetric	4	6317	7700	82.0
Axisymmetric	6	6962		90.4
Axisymmetric	8	6997		90.9
Axisymmetric	10	6998		90.9
Axisymmetric	12	6997		90.9
3-Dimensional	4	6976		90.6
3-Dimensional	6	6974		90.6

The results are also shown graphically in Figure 7.

6.0 Total Strain Results

Based on Section 5, only the highest through-wall element count cases will be further evaluated. As a result, Figures 8 though 10 show the total Von Mises Strain just prior to onset of instability for the 12 through-wall element axisymmetric model and Figures 11 through 13 show total Von Mises Strain for the 6 through-wall element 3-D model.

7.0 Strain Criteria Comparison

The original failure strain criterion described in Section 2.0 indicated that when the through-wall total strain exceeded the uniform elongation percentage, the structure would be considered to have failed. As a check of this criterion, the total Von Mises nodal strains as they varied with pressure were extracted from the middle of the modeled disk at the top, middle and bottom of the wall thickness. The resulting strains were then plotted versus the pressure and compared to the actual burst pressure measured in Reference 3 and the failure pressure as defined by the Failure Criterion in Section 2.0.

From the definition of material properties used in the disk burst test, the uniform elongation for 304 stainless steel was 54% (see Section 3.0). Therefore, the failure of the disk will occur when the through-wall total strain exceeds 54% throughout the thickness.

An examination of the 3 geometries for both the axisymmetric and 3-D modeling can be seen in Figures 14 though 19. The results are further summarized in Table 3.

Table 3
Failure Criteria Comparison

Model Type	Model Geometry	Failure Pressure (psi)		
		Burst Test [3]	Instability	Failure Criteria
Axisymmetric	A	15000	14005	~11000
Axisymmetric	B	6800	6694	~5500
Axisymmetric	C	7700	6997	~5750
3-Dimensional	A	15000	13997	~11000
3-Dimensional	B	6800	6671	~5500
3-Dimensional	C	7700	6974	~5750

8.0 Conclusions

Based on the summary in Table 3 of Section 7.0, the use of the uniform elongation limit as the basis of failure criteria in an elastic-plastic finite element analysis results in conservative failure pressures as compared to actual test results. For the three geometries, the uniform elongation criteria predicted a failure pressure that was in the range of 73% to 84% of the actual failure pressure.

A better prediction of actual failure pressure is the pressure at which numeric instability was reached in the ANSYS program. Assuming a numeric instability criterion, failure pressure would range from 90% to 98% of actual failure pressure.

9.0 References

1) Structural Integrity Calculation W-DB-01Q-301, Rev. 1, "Elastic-Plastic Finite Element Stress Analysis of Davis-Besse RPV Head Wastage Cavity."

2) Email of from B.R. Grambau (Framatome ANP) to N. Cofie (SI), "308 Stress –Strain Curve," March 15, 2002, SI File W-DB-01Q-202.

3) P. C. Riccardella, "Elastic-Plastic Analysis of Constrained Disk Burst Tests," ASME Paper No. 72-PVP-12, Proceedings of Pressure Vessel and Piping Conference, New Orleans, LA, September 17-21, 1972.

4) ANSYS/Mechanical, Revision 5.7, ANSYS Inc., December 2000

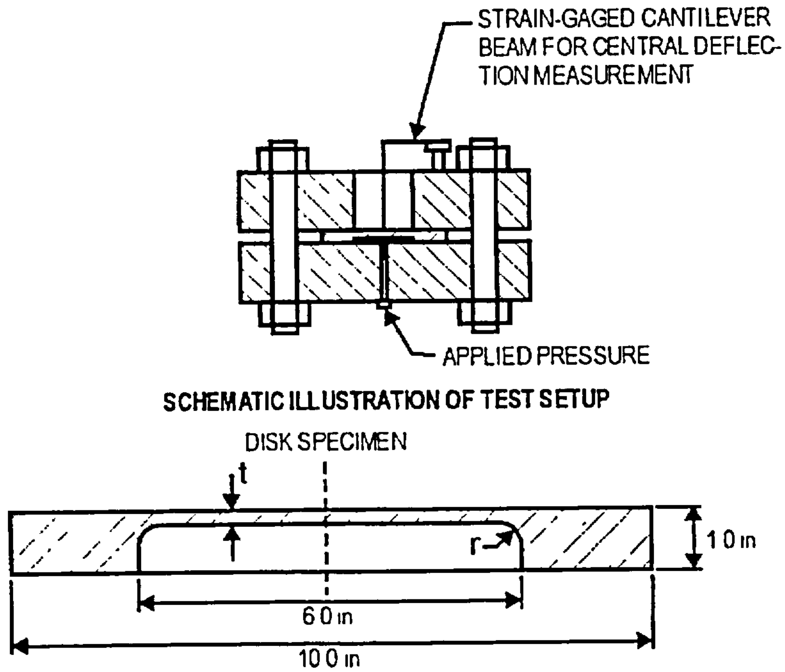

GEOMETRY	THICKNESS (t)	FILLET RADIUS ®
A	0 25 in	0 375 in
B	0 125 in	0 125 in
C	0 125 in	0 375 in

02055R0

Figure 1 – PVRC Disk Test Details (Reference 3)

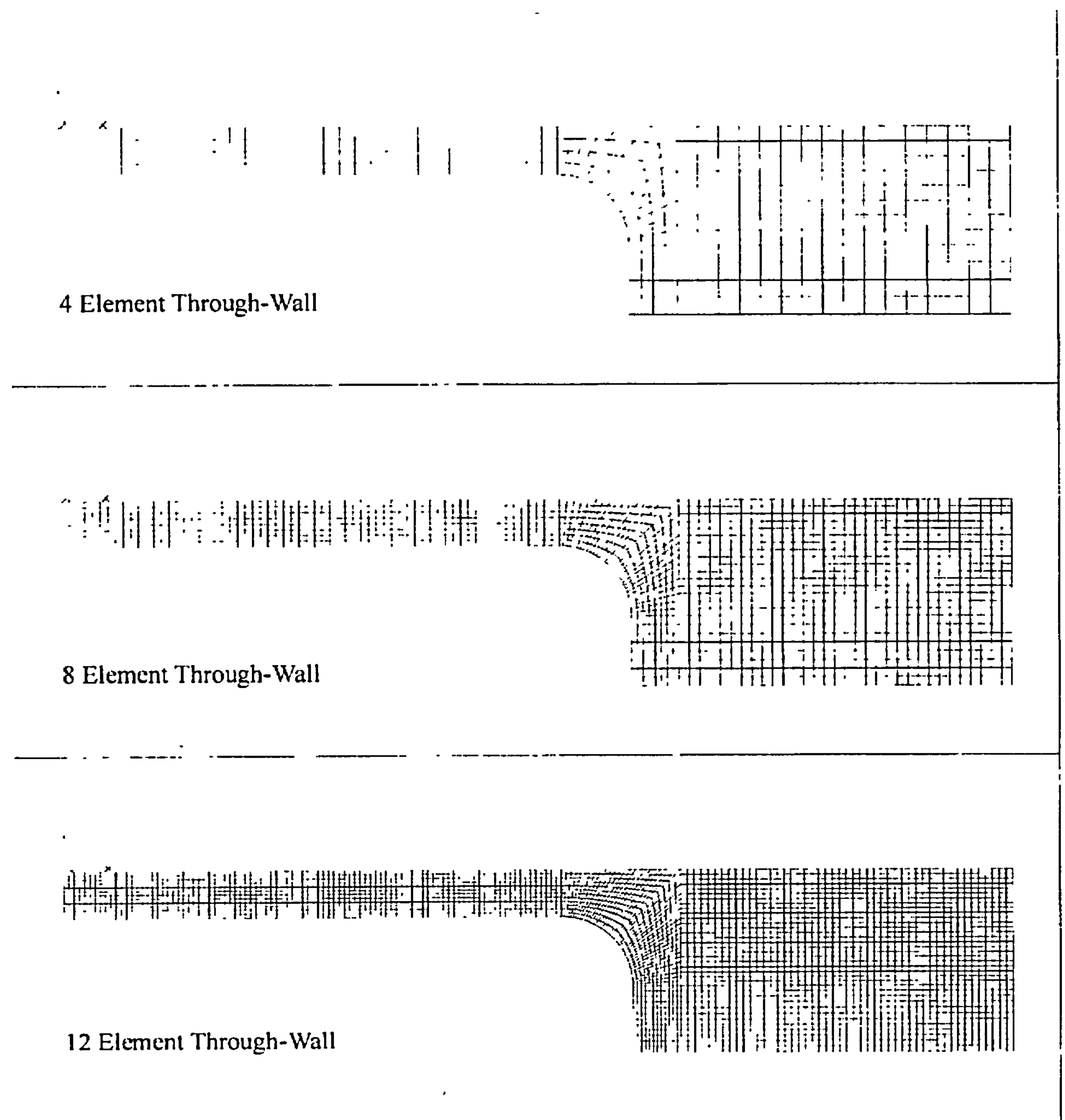

Figure 2 – Mesh Density Example for Axisymmetric Finite Element Model for Geometry-A

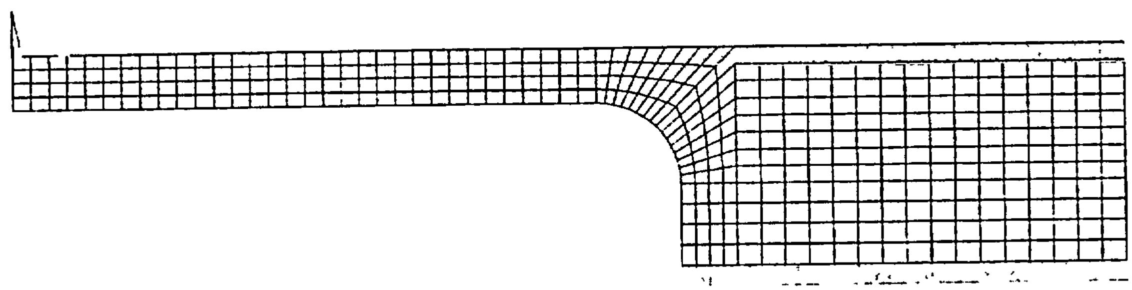

Figure 3 – Mechanical Boundary Conditions Example for Axisymmetric Finite Element Model for Geometry-A

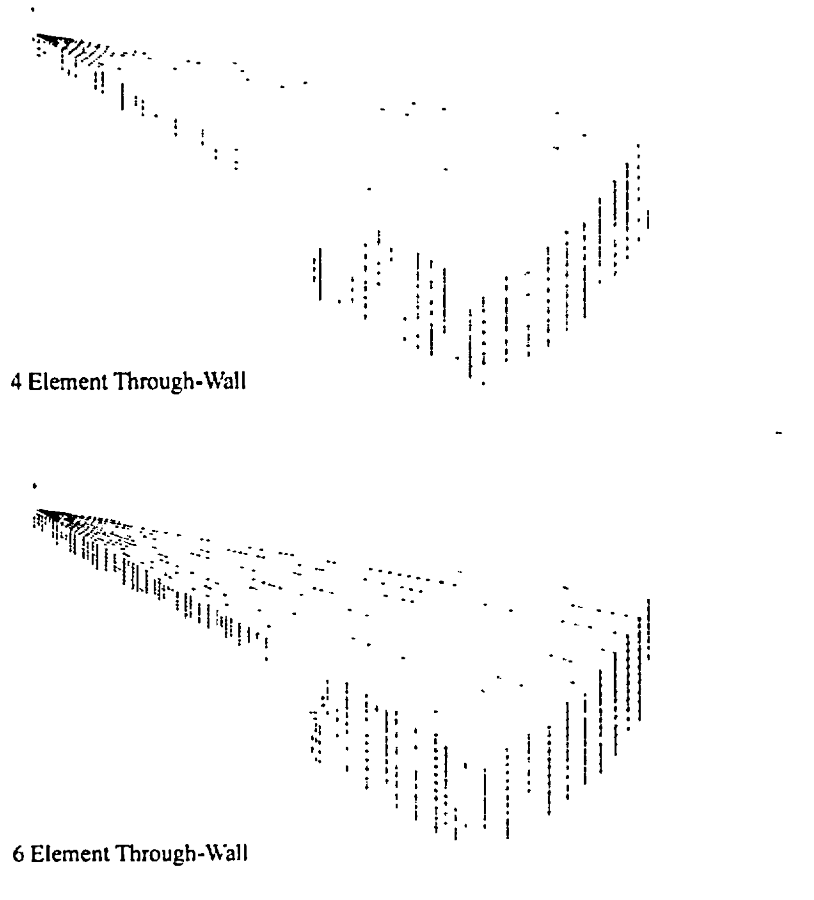

Figure 4 – Mesh Density Example for 3-D Finite Element Model for Geometry-A

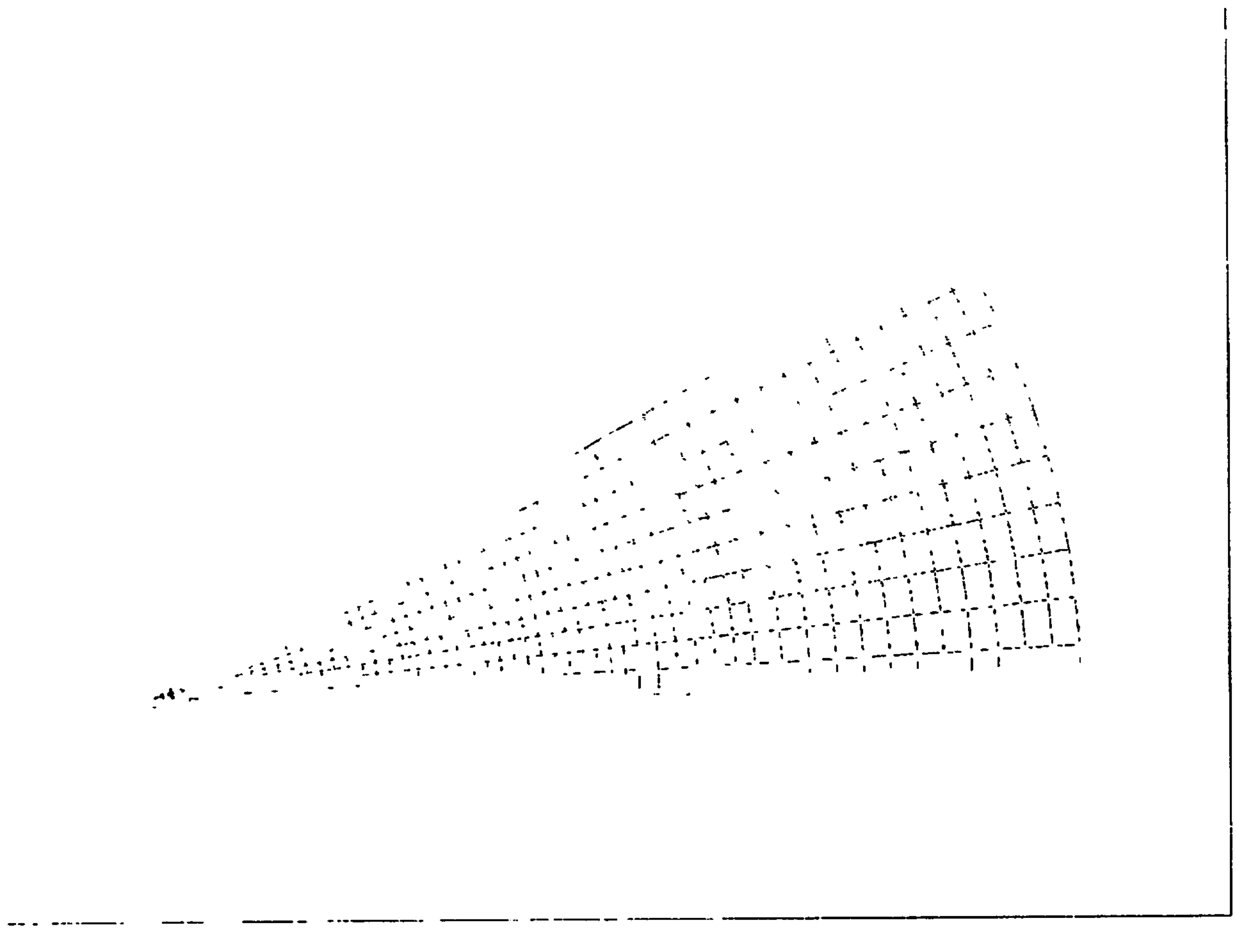

Figure 5 – Mechanical Boundary Conditions Example for 3-D Finite Element Model for Geometry-A

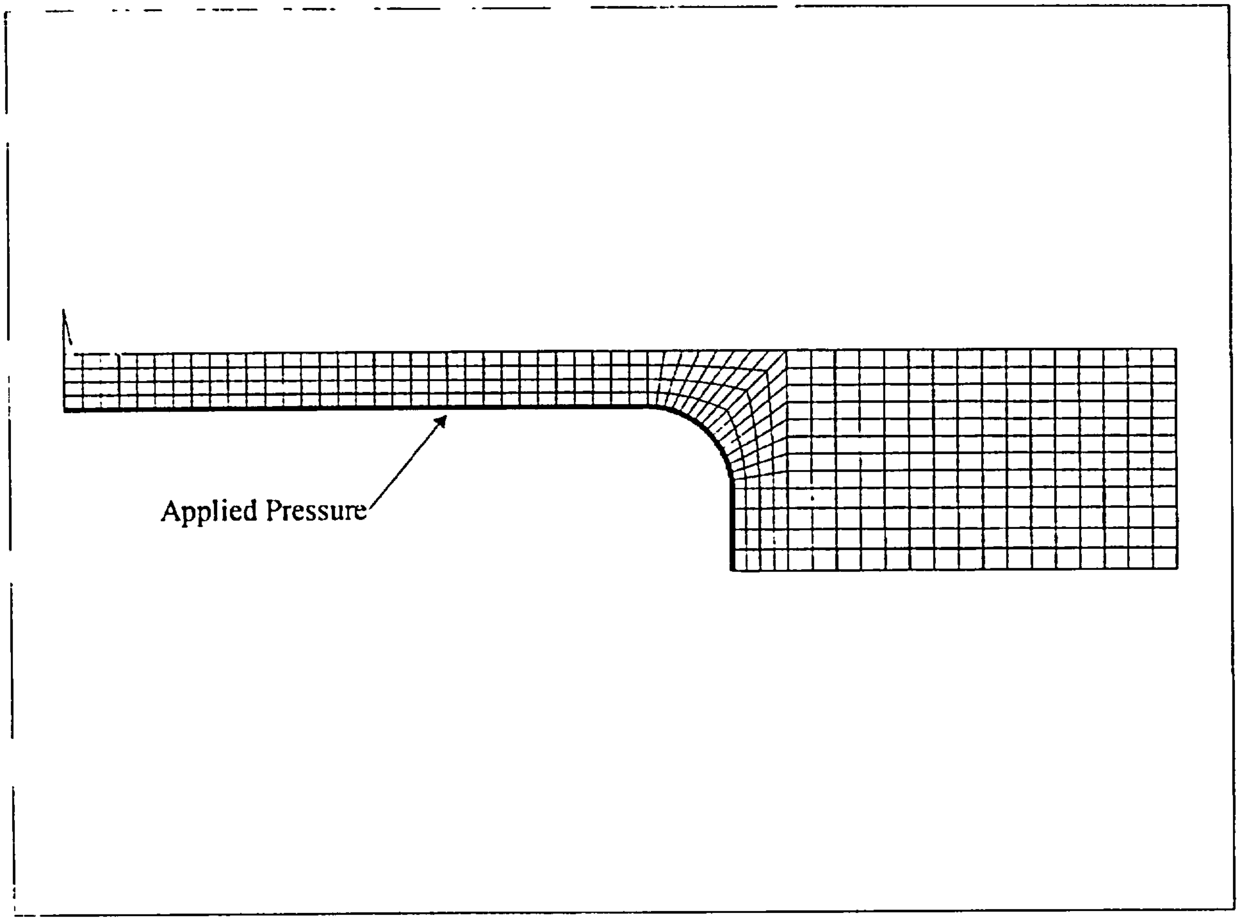

Figure 6 – Applied Pressure Example (Axisymmetric Geometry-A Model)

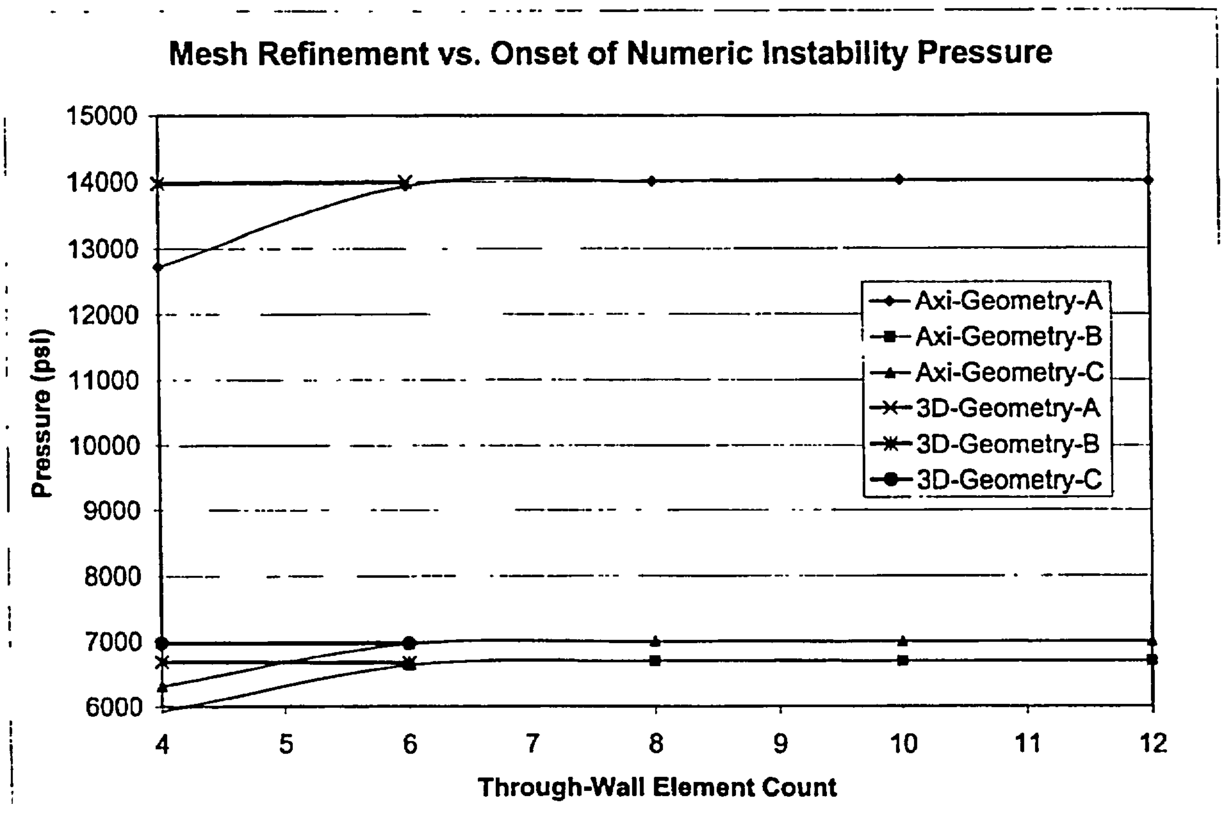

Figure 7 – Mesh Density Effects

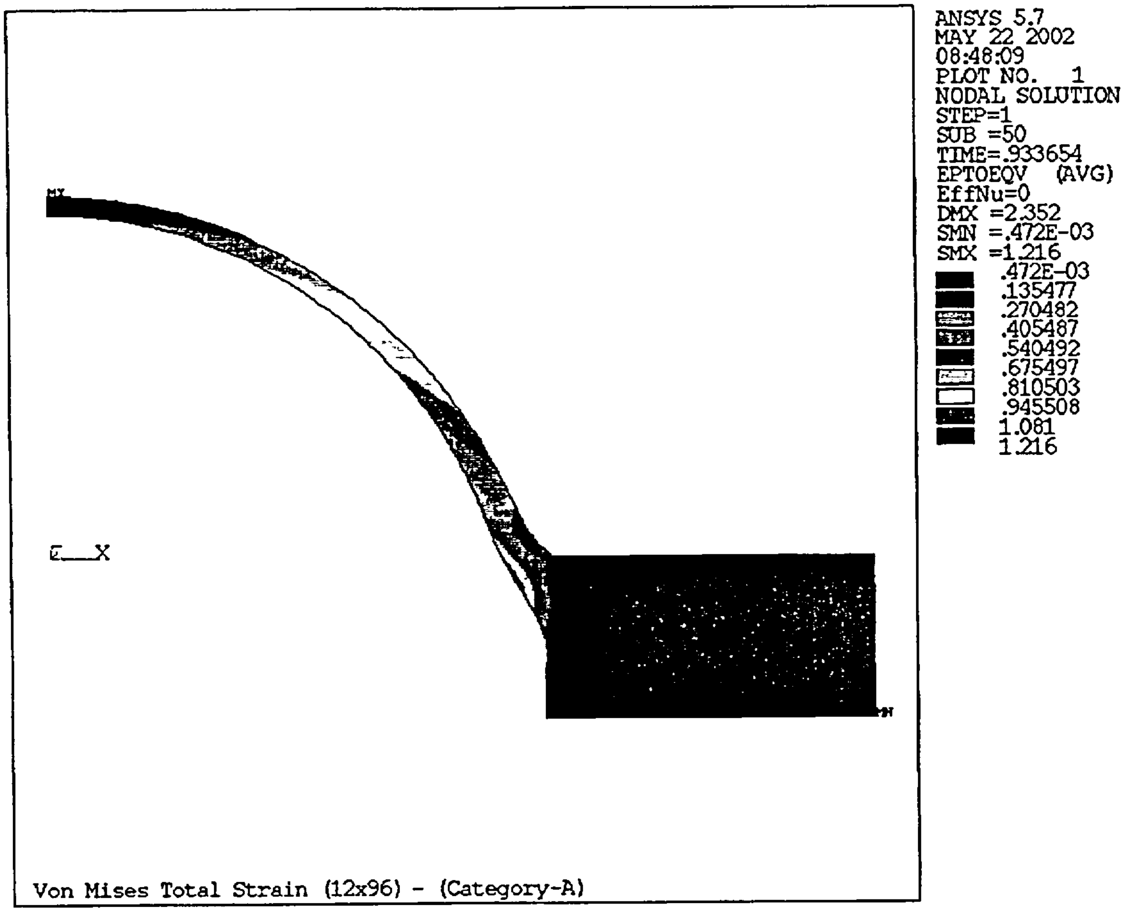

Figure 8 – Total Von Mises Strain Just Prior to Numeric Instability
Geometry-A – Axisymmetric

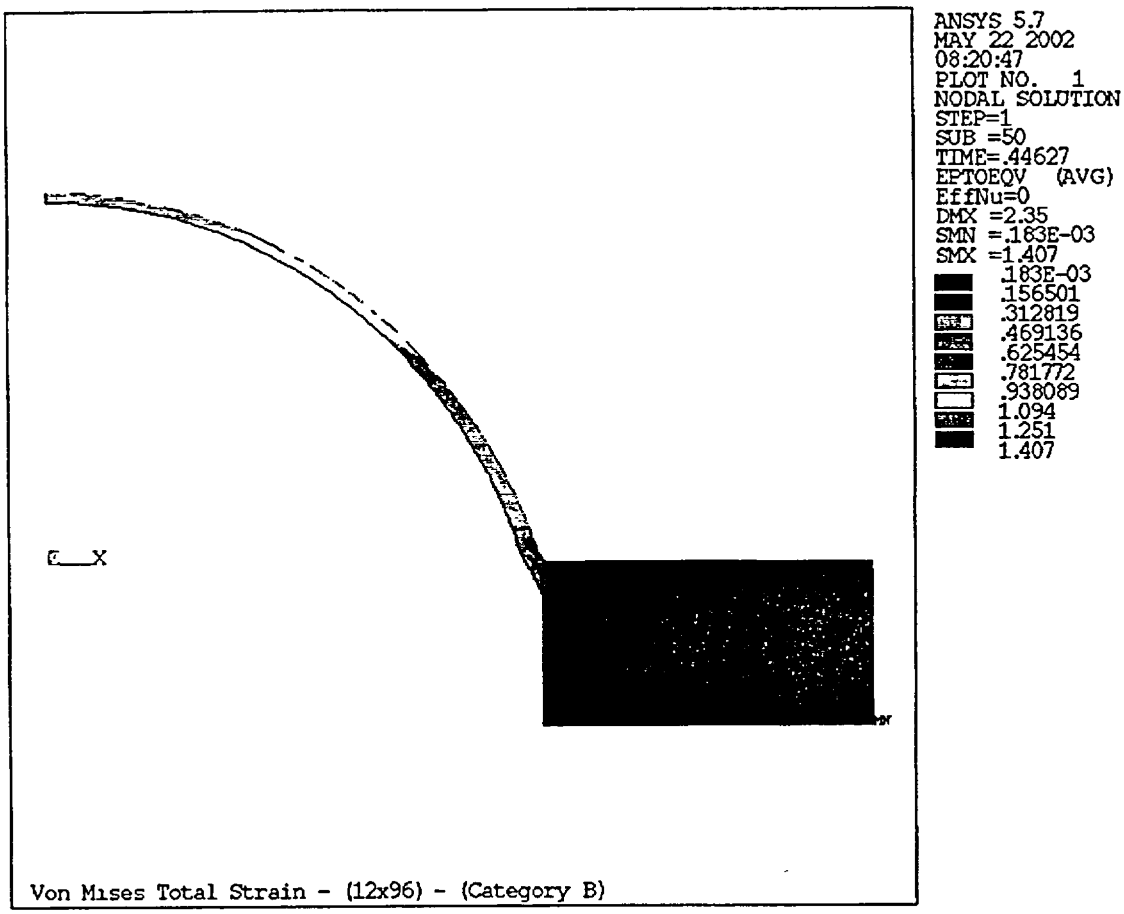

Figure 9 – Total Von Mises Strain Just Prior to Numeric Instability
Geometry-B – Axisymmetric

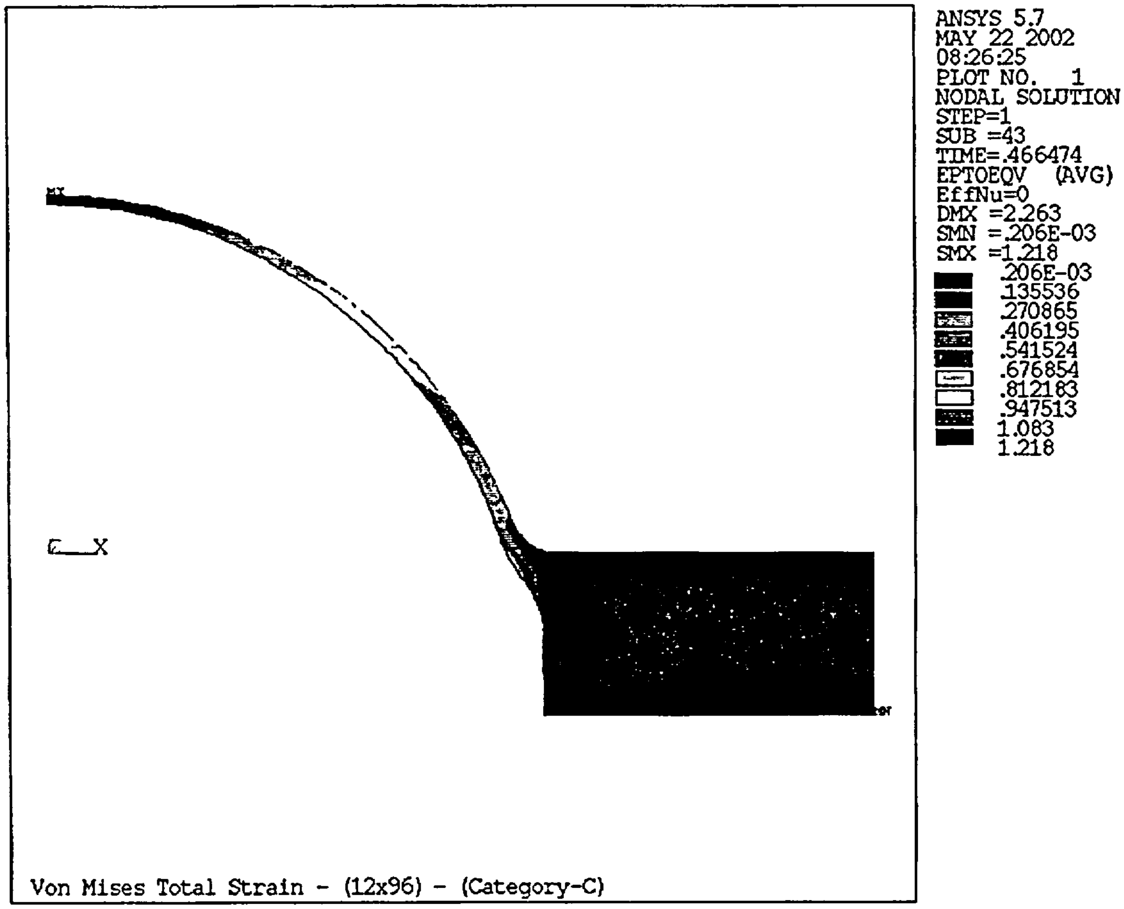

Figure 10 – Total Von Mises Strain Just Prior to Numeric Instability
Geometry-C – Axisymmetric

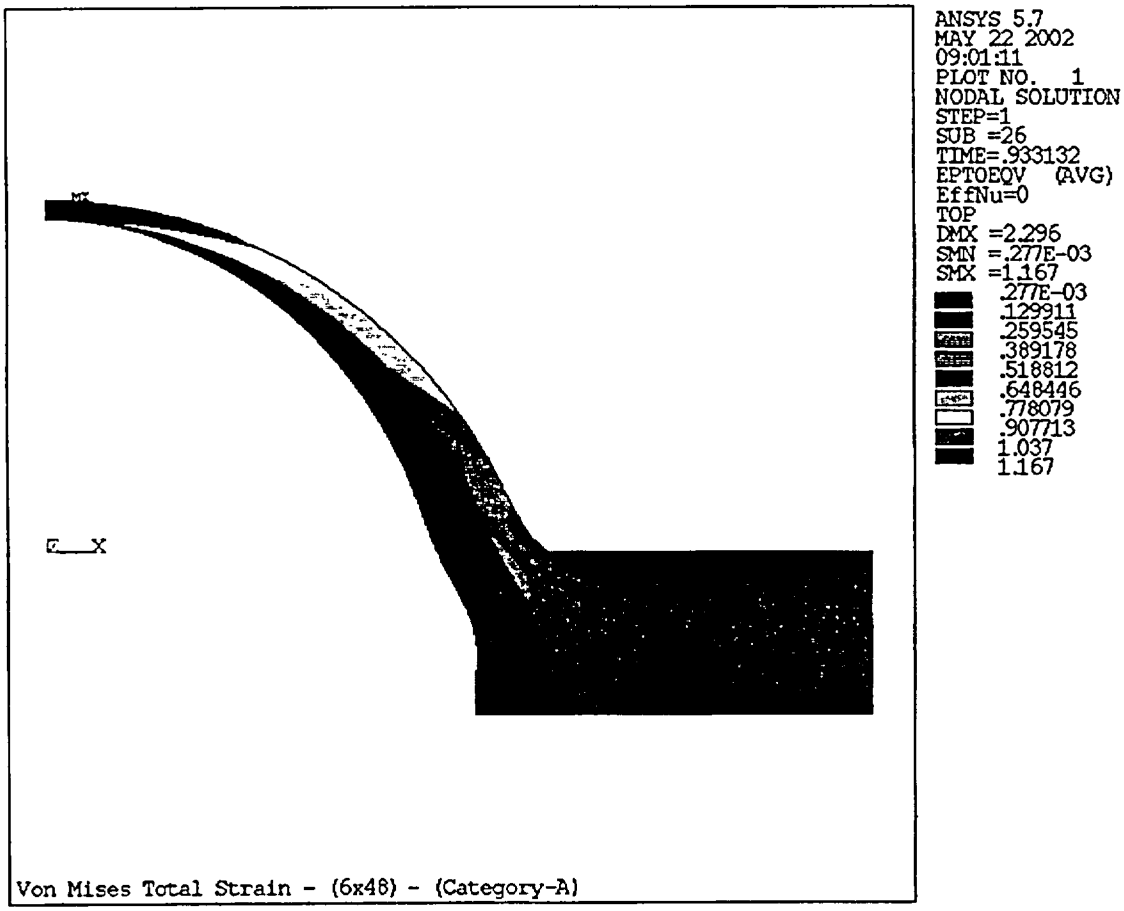

Figure 11 – Total Von Mises Strain Just Prior to Numeric Instability
Geometry-A – 3-Dimensional

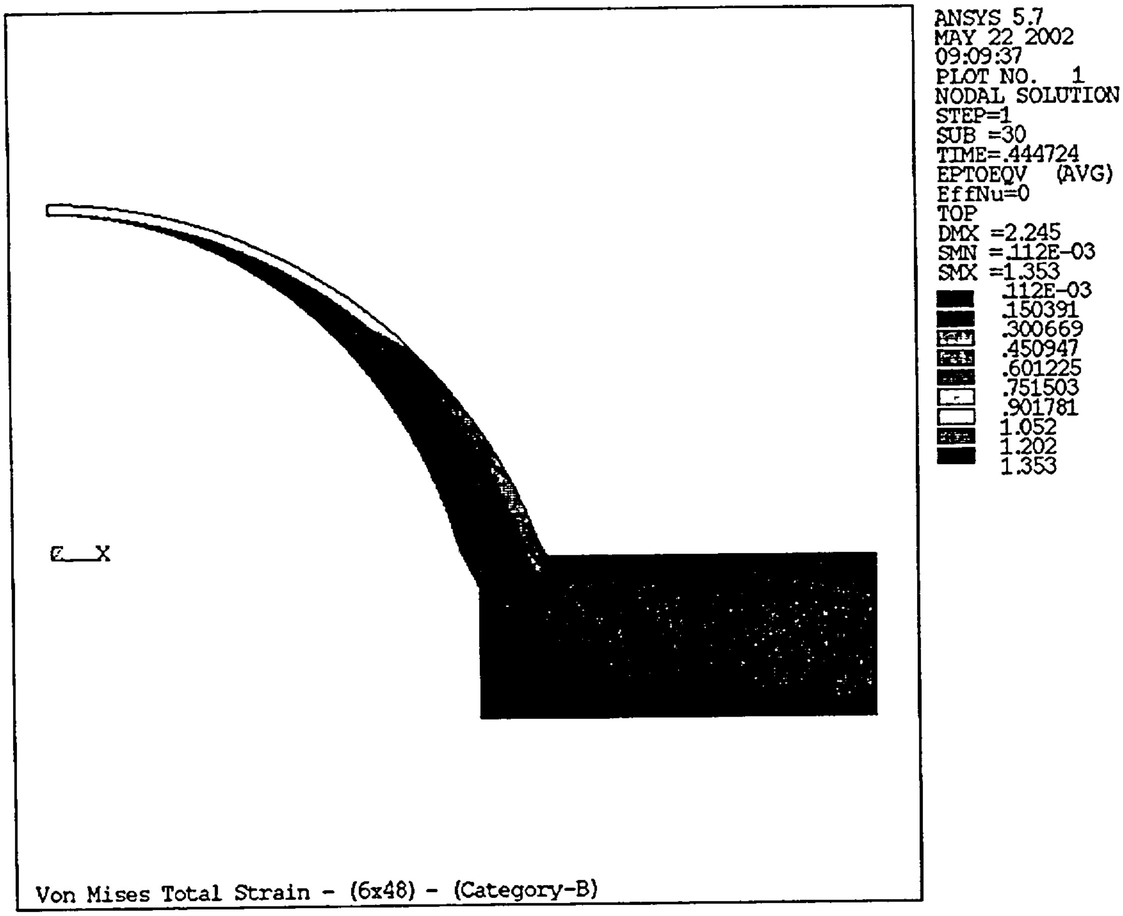

Figure 12 – Total Von Mises Strain Just Prior to Numeric Instability
Geometry-B – 3-Dimensional

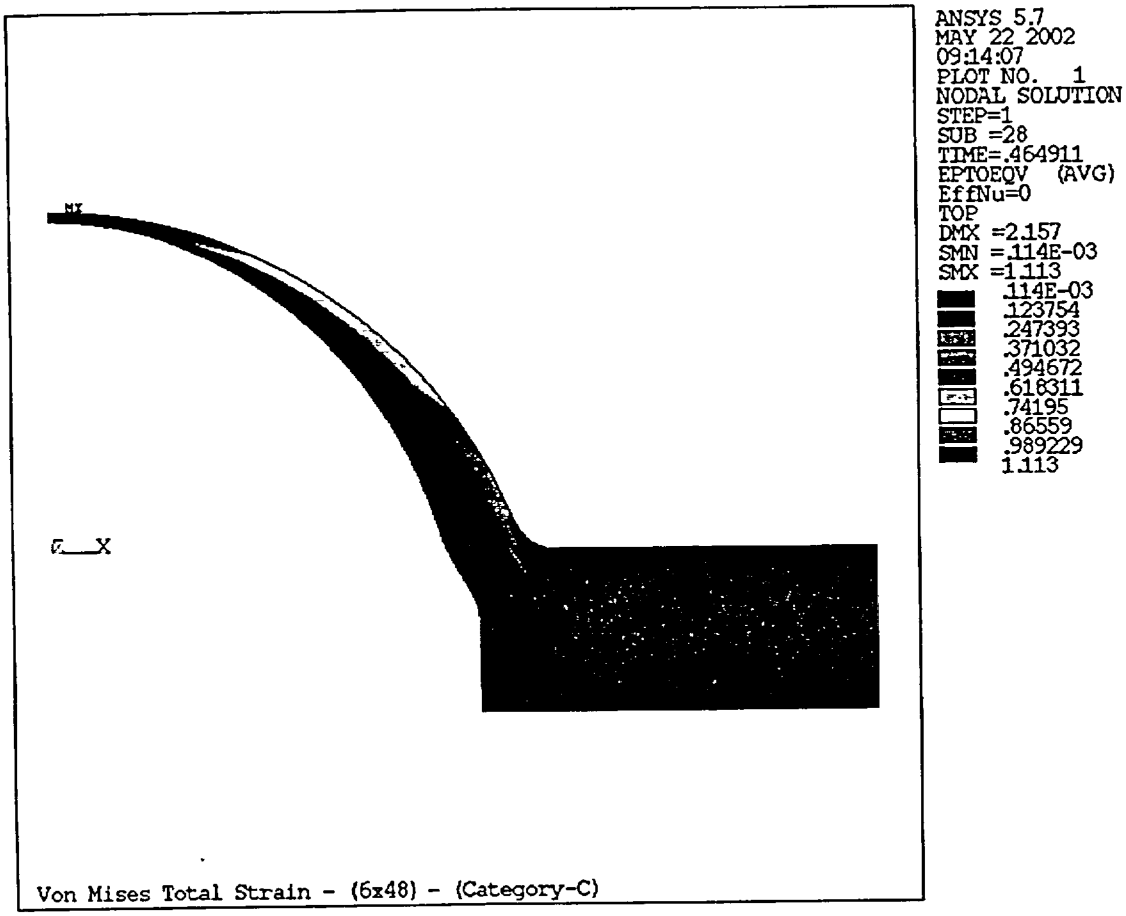

Figure 13 – Total Von Mises Strain Just Prior to Numeric Instability
Geometry-C – 3-Dimensional

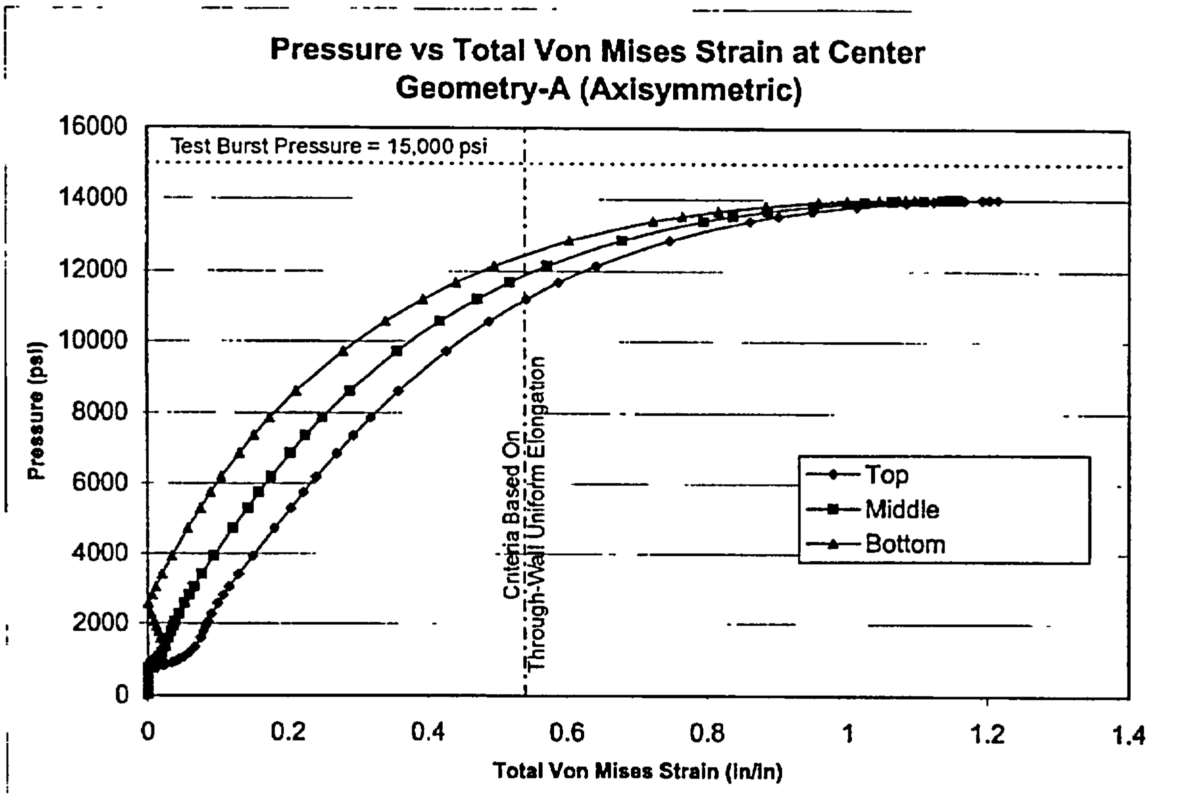

Figure 14 – Through-Wall Strain Results at Center of Disk
Geometry-A (Axisymmetric)

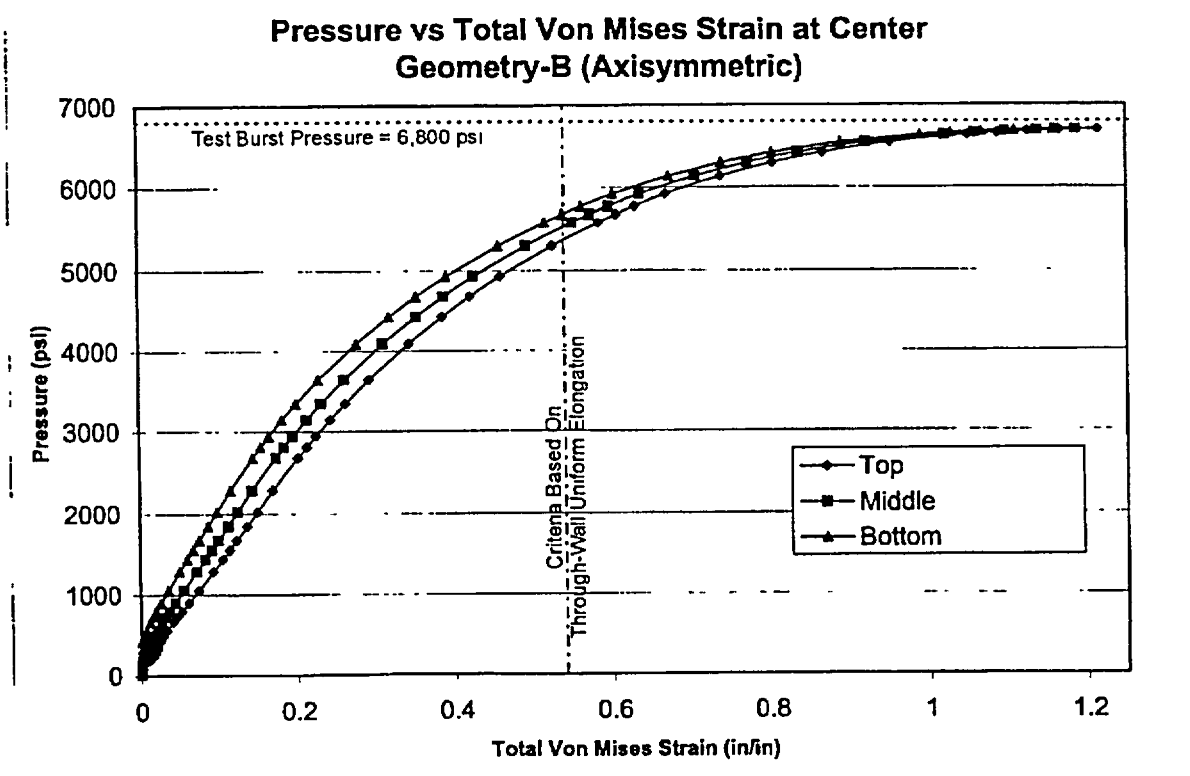

Figure 15 – Through-Wall Strain Results at Center of Disk
Geometry-B (Axisymmetric)

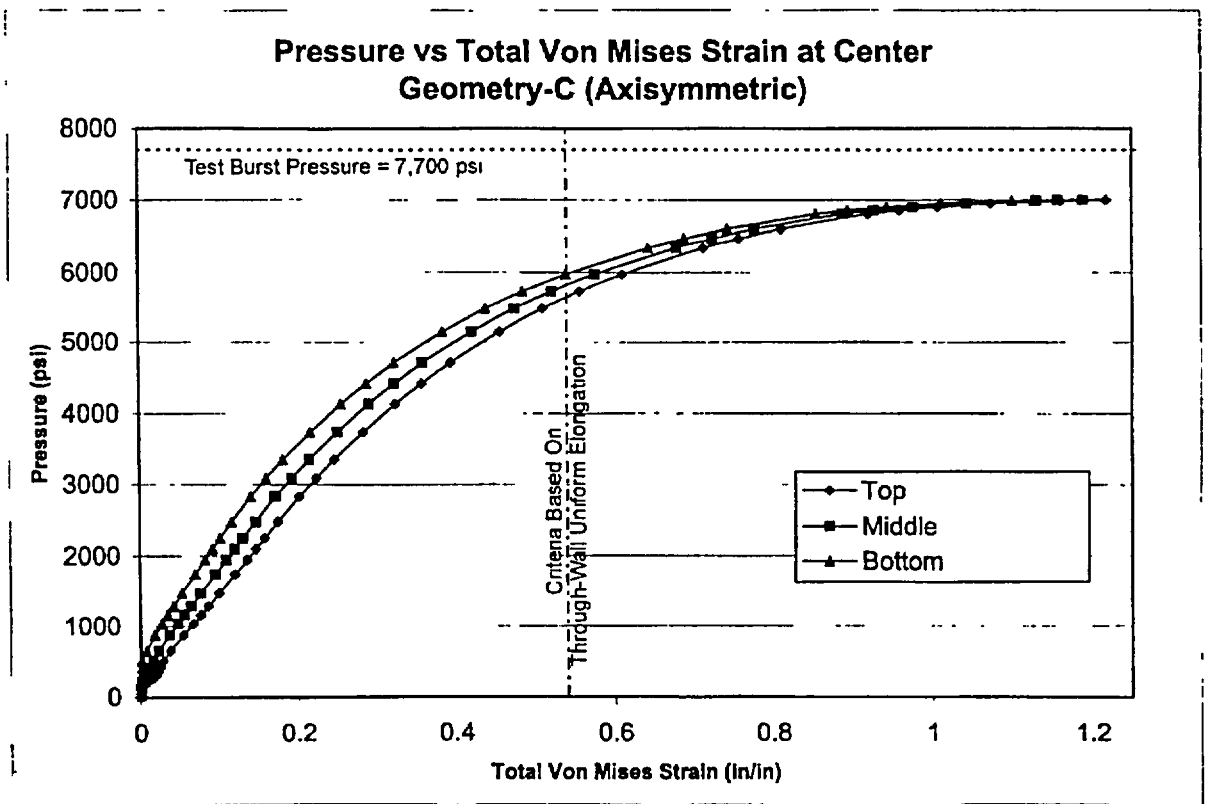

Figure 16 – Through-Wall Strain Results at Center of Disk
Geometry-C (Axisymmetric)

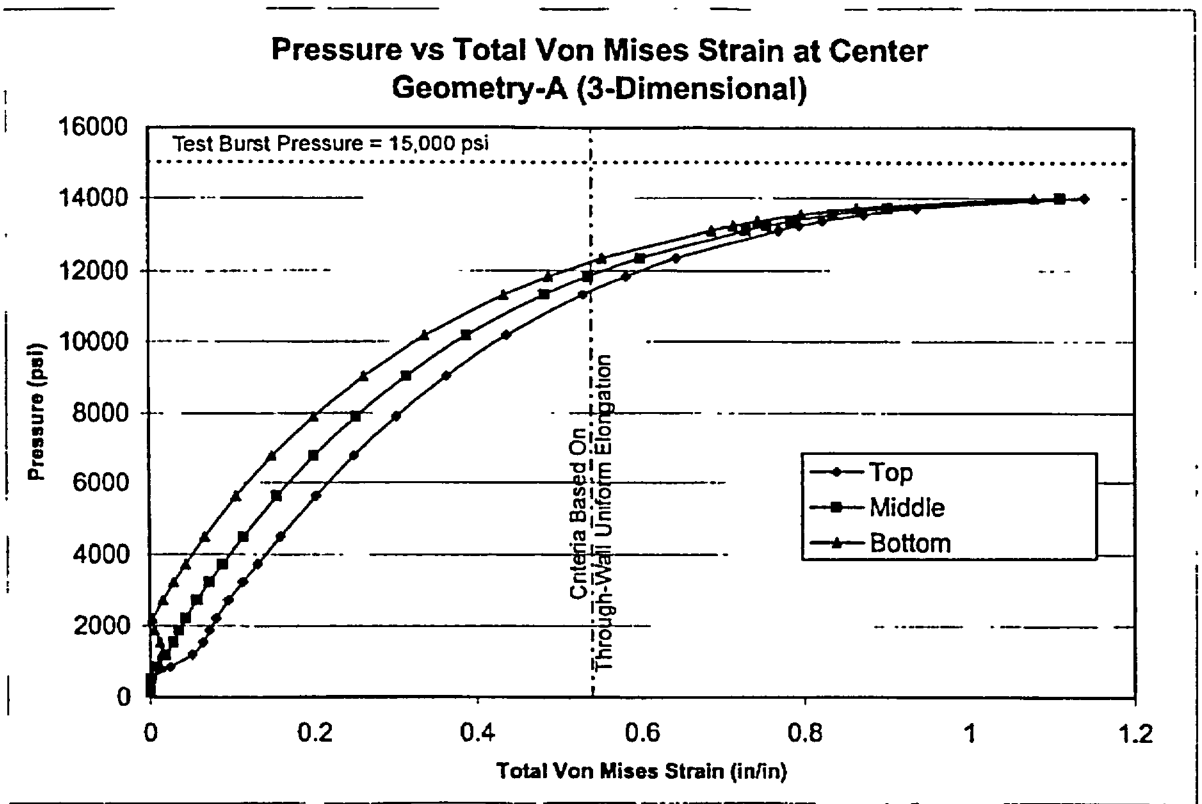

Figure 17 – Through-Wall Strain Results at Center of Disk
Geometry-A (3-Dimensional)

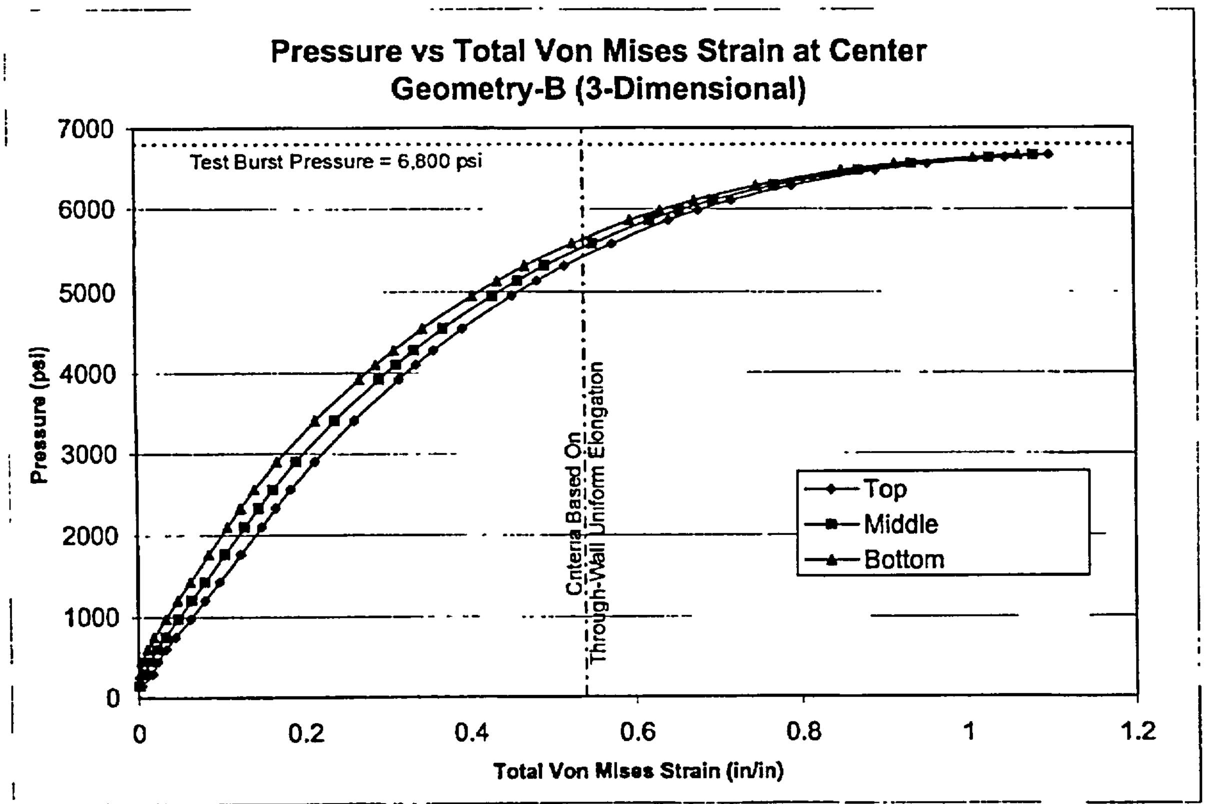

Figure 18 – Through-Wall Strain Results at Center of Disk
Geometry-B (3-Dimensional)

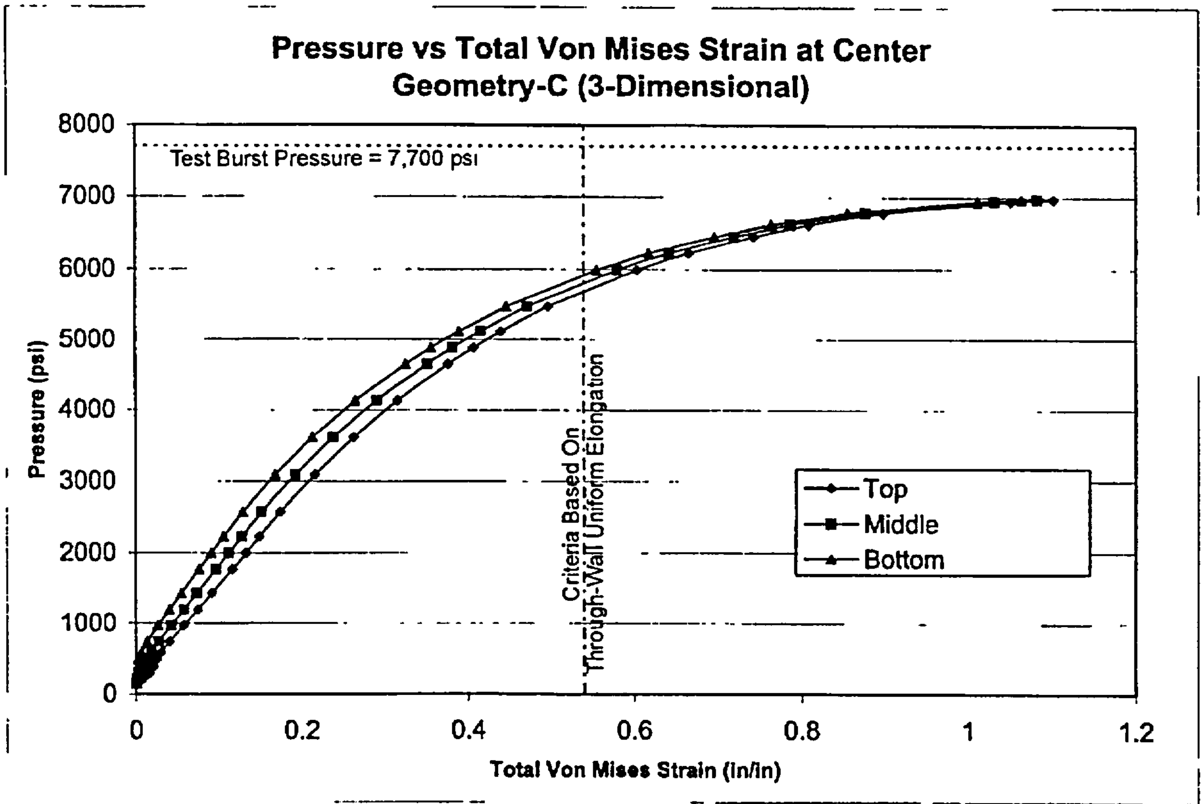

Figure 19 – Through-Wall Strain Results at Center of Disk
Geometry-C (3-Dimensional)

APPENDIX A

NRC Staff Comments and Questions on Davis-Besses Safety Significance Assessment (SIA-W-DB-01Q-301) Submitted April 8, 2002

	Revision	0			
	Preparer/Date	RLB 5/31/02			
	Checker/Date				
	File No. W-DB-01Q-304				Page A1 of A2

NRC STAFF COMMENTS AND QUESTIONS ON DAVIS-BESSE SAFETY SIGNIFICANCE ASSESSMENT (SIA-W-DB-01Q-301) SUBMITTED APRIL 8, 2002

FAILURE CRITERION

(1) What is the technical basis of the failure criterion (e.g., strain exceeding 11.15%) used to determine the failure conditions of the cladding layer? Provide specific technical references in the literature that support the failure criterion used in this evaluation.

(2) How does the failure criterion (e.g., based on ultimate strain in a uniaxial tensile test) account for the effects of biaxial loading in the cladding, or triaxial loading in the cladding at the edges of the degradation cavity?

(3) The failure criterion applied in SIA report W-DB-01Q-301 (e.g., the minimum cross-sectional strain exceeding the failure strain of 11.15%) allows the strain levels in the cladding to exceed the critical strain value entirely through the thickness, leading to very large strains at the surface of the cladding, up to 49% in Table 5 of the SIA report. What is the technical basis for this approach, as opposed to the average cross-sectional strain, or the maximum cross-sectional strain?

(4) Did you explore a continuum damage mechanics analysis to give guidance of the failure criterion once the strains exceed the critical strain where necking/void growth starts? If not, provide the technical basis for not using a continuum damage mechanics analysis. [Poisson's ratio of 0.5 no longer applies once this critical strain level is exceeded, so the analysis is strictly not valid. (Poisson's ratio is continuously changing as the voids grow at the strains beyond the start of necking.) This results in a stress redistribution that is not accounted for in a standard elastic-plastic analysis.]

(5) How would the strain values change if the stress free temperature was assumed to be the stress relief temperature instead of 70°F, and the analysis accounted for the differential thermal expansion of the cladding and head steel at the operating temperature of 605°F?

GEOMETRY/MESHING

(A) Does the size of the degradation cavity and the transition from the cladding thickness to the head thickness that was used in the SIA report reflect current knowledge regarding the cavity geometry, in particular the undercut area described in Figure 13 on page 103 of the Davis-Besse Root Cause Analysis Report (CR2002-0891), dated April 15, 2002? What is the transition geometry assumed in the analyses?

(B) Is there sufficient mesh refinement through the cladding thickness to adequately capture the bending and shear strains at the edge of the cavity? Describe any sensitivity studies used to demonstrate the adequacy of the mesh refinement.

(C) Was the cladding deposited by weld wire? Do the thinner cladding thickness measurements from UT coincide with the locations of weld bead toes? In what direction do the cladding weld beads run relative to the long axis of the degradation cavity?

APPENDIX B

Pressure Vessels and Piping Division Paper No. 72-PVP-12, "Elasto-Plastic Analysis of Constrained Disk Burst Tests"